**P2.7** 

# APPLICATIONS OF AN ELECTRIFIED ONE-DIMENSIONAL CLOUD MODEL

Rachel I. Albrecht [1,*]
Carlos A. Morales [1]
Maria Assunção F. Silva Dias [1,2]
Walt Petersen [3]

[1] *University of São Paulo, São Paulo, Brazil*
[2] *Centro de Previsão de Tempo e Clima, Cachoeira Paulista, Brazil*
[3] *University of Alabama, Hunstville, Alabama*

## 1 INTRODUCTION

Cloud and its precipitation play a fundamental role in the evolution of weather processes. For example, weather is commonly characterized by a wide range of cloud and precipitation types including rain, hail and snow. Clouds are the result of complex interactions of a large number of processes, e. g., moist convection, turbulence, vertical motion, and microphysics of hydrometeors. In order to produce a reliable weather forecast it is essential to include these weather elements in numerical weather prediction models. These models are capable to produce thunderstorms, that is, clouds that are electrified enough to produce lightning. However, current weather forecast cloud models are limited to the production of hydrometeors and its associated precipitation, and do not include the electrification processes that produces lightning.

Lightning can cause severe damage to properties and lives. More people are killed by lightning than by tornadoes, and it is estimated that lightning damages cost more than 4 billion dollars for the North Americans in fires suppressing, insurances, aircrafts mishaps and upsets, electrical infrastructure, and electronic components, and 30% of power outages are caused by lightning strikes (from the *Department of Transportation, Federal Aviation Administration*). The addition of hydrometeor electrification processes into a numerical cloud model would make reliable lightning forecasts and help to diminish lightning related damages.

Determining how a thunderstorm become electrified has been a goal of laboratory experiments and field observations for several decades (MacGorman and Rust, 1998). Investigators had made substantial progress evaluating various electrification processes, and have found one type of process that appears capable of producing maximum electric filed magnitudes comparable of those observed in nature (Takahashi, 1984; Saunders et al., 1991; Williams et al., 1994), which is discussed in next section. However, observations of myriad electrical properties of thunderstorms remain unexplained. The reason for this is that it is nearly impossible to sample adequately all processes important to thunderstorm electrification because (MacGorman and Rust, 1998): i) relevant scales range from properties of ions and water particles to wind patterns and particle trajectories; ii) storms are complex and can change drastically in a few minutes, so differences in the time and location of which various properties are measured often interfere with analysis of causality; and iii) access for measurements is limited because clouds are remote from ground and many regions inside the cloud are hostile to instrumentation, aircraft and balloons. Therefore, one powerful and possible instrument to test laboratory and theoretical hypothesis of thunderstorm electrification is also the simulation of electrified clouds using numerical weather prediction models.

As numerical modeling of electrified thunderstorms can be helpful in scientific and social frameworks, this paper presents the preliminary results of a electrified 1D cloud model. As a first application, this model is being used to investigate the continental and maritime behaviors of the convective systems at the Amazon region along the year that modulate the lightning records, with two maximum records in both the onset and break periods of the monsoon (Williams et al., 2002). These characteristics of number of lightning for a thunderstorm in different periods of the year *can be only* driven by the large-scale and thermodynamic conditions of the atmosphere. This effect works on the updraft strength given by the larger cloud buoyancy (also known CAPE – Convective Available Potential Energy, and CINE - Convective Inhibition Energy), which leads to stronger continental updrafts, invigorating the ice microphysics favorable to charge separation and lightning. However, during the dry-to-wet season, local farmers prepare the agriculture pasture by burning it. These fires release high quantities of aerosols to the atmosphere, contributing to the

* *Corresponding author address:* Rachel I. Albrecht, Department of Atmospheric Sciences, University of São Paulo, São Paulo, SP 05508-090 Brazil; e-mail: rachel@master.iag.usp.br

increase of the cloud condensation nuclei (CCN). This increase in CCN concentration at the boundary layer *can also be* an important additional parameter for characterizing the convection, known as the aerosol hypothesis of Rosenfeld (1999) and Williams et al. (2002), once by coincidence or not the high CCN counts occurred during the two maximum lightning record periods.

Knowing the fact that the lightning records are strongly dependent on the season of the year, this paper presents a preliminary work on the investigation of the contribution of the thermodynamics only (CAPE and CINE) on the thunderstorm life cycle of local convection over southwest Amazon. In section 2, there is a brief description of the one-dimensional cloud model, focusing on the microphysical processes of hydrometeors and electrification of clouds. Section 3 presents the first results in modeling electrified clouds, and comparing the results with observational data collected during the two main campaigns inside Large Scale Biosphere-Atmosphere Experiment in Amazonia (LBA) held in the state of Rondonia, Brazil. In the last section, we summarized the findings and offered discussion remarks and perspectives.

## 2 THE ELECTRIFIED 1D CLOUD MODEL

One-dimensional cloud models have been criticized for exhibiting inconsistencies when tested against real situations. However, their relative simplicity and low computational requirements make these models still valid for several applications. For example, 1D cloud models are useful for studying the implementation of new processes into microphysical cloud parametrization, and three-dimensional cloud models remain computationally cumbersome and expensive for studies that require many model simulations. These facts illustrate the continuing desirability to obtain a one-dimensional cumulus model that is internally consistent and captures the essence of cloud structure (Ferrier and Houze, 1989; Cheng and Sun, 2002, 2004).

The cloud model used in this work is based on a cumulonimbus convection of the dynamic model of Ferrier and Houze (1989), coupled with the ice classes of Ferrier (1994) and Petersen (1997), and a parametrization of charge transfer between classes of hydrometeors. In the following subsections, there is a brief description of the model equations and governing physics.

### *2.1 Dynamic equations*

The behavior of a parcel of moist air in a cloud is described by an equation of motion, thermodynamic equations, and continuity equations. This 1D cloud model is formulated in cylindrical coordinate system (*r, l, z*) and is axial symmetric, with variable radius. All dependent arbitrary variable $A$ is defined as deviations from the their environment ($A_e$) values and the quantity within the cloud ($A_c$), expressed as:

$$A_c = A_e + A \quad (1)$$

The model predicts cloud-averaged values of vertical velocity $\overline{w}$, potential temperature $\overline{\theta}$, pressure perturbation relative to the large-scale environment, mixing ratios[1] $\overline{q_x}$ and charge densities[2] $Q_x$ of $x$ water classes: water vapor (*v*), cloud water (*cw*), rain (*r*), ice crystals (*i*), snow flakes (*s*), graupel (*g*) and hail stones (*h, D*>2 cm).

The prognostic equation for the arbitrary variable $A$ in cylindrical coordinates is

$$\frac{dA_c}{dt} = \frac{\partial A_c}{\partial t} + \frac{1}{r}\frac{\partial (r\,u\,A_c)}{\partial r} + \frac{1}{\rho_e}\frac{\partial (\rho_e\,w\,A_c)}{\partial z} \quad (2)$$

where $u$ is the radial velocity $dr/dt$, $r_e$ is the density of environment, and $w$ is the vertical velocity. An horizontal integration is performed to reduce the equations from three dimensions to one. The horizontal area-average value $\overline{A}$, the deviation from horizontal area $A'$, the lateral boundary average $\tilde{A}$, and the deviation from the lateral boundary average $A''$ are defined as

$$\overline{A} = \frac{1}{\pi R^2}\int_0^{2\pi}\int_0^R A\,r\,dr\,d\lambda \quad , \quad A' = A - \overline{A}$$
$$\tilde{A} = \frac{1}{2\pi}\int_0^{2\pi} A\,d\lambda \quad , \quad A'' = A - \tilde{A} \quad (3)$$

By averaging (2) over the cell's horizontal area, making use of (3), mass continuity equation, and neglecting small changes with time in the properties of the large-scale environment, we obtain

$$\begin{aligned}\frac{\partial \overline{A}}{\partial t} = &-\frac{\partial A_e}{\partial t} - \overline{w}\frac{\partial A_e}{\partial z} + \underset{(i)}{\overline{\frac{dA_c}{dt}}} \\ &+ \underset{(ii)}{\frac{\tilde{A}}{\rho_e R^2}\frac{\partial(\rho_e R^2 \overline{w})}{\partial z}} - \underset{(iii)}{\frac{1}{\rho_e R^2}\frac{\partial(\rho_e R^2 \overline{wA})}{\partial z}} \\ &- \underset{(iv)}{\frac{2}{R}\left(\widetilde{u''A''} - \widetilde{w''A''}\frac{\partial R}{\partial r}\right)}\end{aligned} \quad (4)$$

Term (i) in (4) represents the sources and sinks of the dependent variable $\overline{A}$; it takes on the following forms in the equations for vertical momentum and

1 Grams of $x$ per kilogram of air.

2 Charge per unit volume.

thermodynamic energy respectively:

$$\frac{\overline{dw}}{dt}=\overline{B}-R_d\theta_{ve}\frac{\partial\overline{P}}{\partial z} \qquad (5)$$

$$\begin{aligned}\frac{\overline{d\theta}}{dt}=&\frac{L_v}{\tau C_p}(q_{cw}[condensation]-q_r[evaporation])\\ +&\frac{\delta L_s}{\tau C_p}\sum_x q_x[nucleation, deposition, sublimation]\\ +&\frac{L_f}{\tau C_p}\sum_x q_x[freezing, melting]\\ +&\frac{L_f}{\tau C_p}\delta q_{cw}[collection, freezing]\end{aligned} \qquad (6)$$

where $\overline{B}$ is the buoyancy term, $R_d$ is the dry gas constant, $q_{ve}$ is the equivalent virtual potential temperature, $\overline{P}$ is pressure, $L_v$, $L_s$ and $L_f$ are, respectively the latent heat of vaporization, sublimation and fusion, $t$ is the Exner function, $C_p$ is the specific heat of air at constant pressure, $q_x$ are the mixing ratio of the $x$ water classes at the model, and $d$ has the value of 1 if the temperature $T$<0ºC, and 0 otherwise.

For mixing ratios $q_x$ and charge density $Q_x$, term (i) in (4) is given by the sources and sinks of all possible interactions between the $x$ water classes:

$$q_x=\sum(sources\ of\ x)-\sum(sinks\ of\ x) \qquad (7)$$

$$Q_x=\sum(sources\ of\ x)-\sum(sinks\ of\ x) \qquad (8)$$

The interactions considered in mixing ratios (7) are condensation, evaporation, aggregation, rimming, breakup, etc, and those for charge densities (8) are explained in next subsection.

In (4), there are two contributions to the net entrainment of air into convective cells from their sides: term (ii) represents the horizontal inflow of air needed to satisfy mean mass continuity, and term (iv) represents the turbulent mixing of air from the immediate environment into the convective cores without the net exchange of mass across cell boundaries. Term (iii) is also a turbulent mixing parametrization, but for the vertical transport. More details on the retrieving of dynamic equations and parametrization of each term in (4) can be found in Ferrier and Houze (1989), Cheng and Sun (2002, 2004), and details on the microphysical processes can be found in Ferrier (1994) and Petersen (1997).

### *2.2 Electrification equations*

The magnitude of charge that electrification mechanisms place on a precipitation particle can range from zero to more than 100pC. The main key hypothesized cloud electrification mechanisms are the ion capture, and inductive and noninductive rebounding particles mechanisms. The ion capture mechanism suggests that precipitating hydrometeors would become polarized in an electric field, and if they fall relative to ions moving under the influence of both wind and electric field, ions of the same sign of the bottom of the hydrometeors are repelled and ions of the opposite sign are attracted and captured. In the inductive rebounding particles mechanism, the precipitation particle is polarized by the ambient field, and when the falling precipitation collides with a cloud particle (also polarized), some of the charge on the bottom of precipitation particle transfers to the cloud particle. If the cloud particle rebounds, it will carry away the charge it has gained and leave behind an excess of the sign of charge that is on the top of the particles. However, the fair weather electric field cannot polarize and make reliable an electrification of clouds in the initial stages (MacGorman and Rust, 1998; Williams et al., 1994). Therefore it might have another mechanism that can first produce a strong enough electric field to make polarized particles. This mechanisms is suggested to be the noninductive rebounding particles (MacGorman and Rust, 1998; Williams et al., 1994).

The noninductive mechanisms are those that do not require a polarization of hydrometeors by an electric field. Of the various types of noninductive mechanisms that are possible, the graupel-ice mechanism is the only one thus far that detailed laboratory and modeling studies have suggested is capable of causing clouds to become electrified enough to be thunderstorms, although other mechanisms also may make significant contributions. Takahashi (1978) for example, found that the magnitude and sign of the charge (*dm*) deposited on a graupel particle depended on temperature and liquid water content. Williams et al. (1994) also added the fact that charge transfers without the presence of an electric field can be possible due to the growth stage of hydrometeors (e. g., deposition, evaporation) , the electrical double layer and the quasi-liquid layer (Baker et al., 1987, and Baker and Dash, 1994).

The parametrization of sources and sinks of charge densities for the $x$ classes of hydrometeors in (8) are based on the Takahashi (1978, 1984) laboratory observations of graupel-ice collisions, being a noninductive charging mechanism. Per unit time, the volume in which a particle $x$=1 of diameter $D_1$ collides with a particle $x$=2 of diameter $D_2$ is given by the *collision kernel* $K_{12}$, and number densities ($n_N$) of the $N$th particle type of diameter $D_N$, that is

$$\frac{\partial Q_1}{\partial t} = \int\int K_{12} n_1(D_1) n_2(D_2)(\delta\mu) dD_1 dD_2$$
$$= -\frac{\partial Q_2}{\partial t} \quad (9)$$

The collision kernel is the effective cylindric volume for collision of particles 1 and 2 times the collision separation efficiency of these two particles $x_{12}$ (which is the fraction of particles 1 in this volume that collide with particle 2 and separate from it), that is (MacGorman and Rust, 1998)

$$K_{12} = \frac{\pi}{4}(D_1 + D_2)^2 |v_1 - v_2| \xi_{12} \quad (10)$$

where $v_1$ and $v_2$ are particles 1 and 2 terminal fall velocities. The size distribution $n_N$ is assumed to have an exponential distribution for graupel and snow, and since cloud ice typically has a narrow distribution, it can be approximated as a population with a single diameter $D_i$. For cloud ice, because $D_i << D_g$ and $v_1 << v_2$, the magnitude of sums and differences of these quantities can be approximated as $D_g$ and $v_g$ in (10). The terminal fall velocities can be approximated to power laws, such as $v_g = a D_g^b$, and the amount of charges transferred (dm) are taken from Takahashi (1978).

Once the model starts to electrically charge hydrometeors, it is necessary to include a lightning parametrization. A primary purpose of lightning parameterizations is to limit the electric field $E$ magnitudes to observed values. Without a lightning parametrization, $E$ would build to unrealistic large values, several times what is needed to cause electrical breakdown of air. Therefore, calculating $E$ at each grid point and if any overpass an adopted limit, a lightning occurs. In this work, it was considered the *breakeven electric field*, that is the threshold electric field necessary for the average kinetic energy of an energetic electron (1 MeV) to remain constant as it gains energy from the electric field and loses energy to collisions (Marshall et al., 1995). The breakeven electric field $E(z)$ ($kVm^{-1}$) decreases with altitude $z$ (km), and contain a model of vertical distribution of the mass density of air, $r_A$ ($kgm^{-3}$) (Marshall et al., 1995):

$$E(z) = \pm 167 \rho_A(z)$$
$$\rho_A(z) = 1.208 \exp\left(-\frac{z}{8.4}\right) \quad (11)$$

At this current version of the model used in this work, there is just one lightning. The next step will be to include a scheme to reorganize charge densities and make several lightnings, reproducing then a thunderstorm life cycle.

## 3 RESULTS

It is presented here two case studies of simulations with initial thermodynamic conditions given by two radiosondes launched at Ouro Preto d'Oeste, RO, Brazil, representing the wet and transition seasons.

It appears that the dominant means by which deep tropical convective clouds are initiated are the lifting of low-level air near the surface by gust fronts associated with cumulus convection that is already present (Ferrier and Houze, 1989). This is period of low level forcing is needed to simulated maximum cloud-top heights consistent with those observed in nature. Therefore, the simulation was conducted using a low level profile of vertical velocity $\overline{w}$ as in Ferrier and Houze (1989), simulating a gust front forcing, which lifts the air to higher levels and initiate the cloud. The vertical profile of $\overline{w}$ increases parabolically from 0 $ms^{-1}$ at the surface to 2 $ms^{-1}$ at $z$=600 m. This low level forcing increased linearly with time during the first 100 s and remained at full strength for the next 1100s. After the first 20 minutes, the forcing was no longer applied. The simulation was conducted for 90 minutes with a time step of approximately 5 s (Ferrier and Houze, 1989), and the vertical resolution of the model is $\Delta z = 200$ m. The very weakness of this lifting gust front considered in these simulations are done to see the real action of the thermodynamics in the lower boundary layer. In the future, stronger lifting gust fronts will be studied to simulate some the effect of high elevations of the terrain (topography).

The first case study to be analyzed is the simulation ran with a radiosonde launched during the break period of the monsoon (Rickenbach et al., 2002) on 1200 UTC 07 February 1999 (Figure 1a). This thermodynamic situation is characterized by a very wet situation, with a 0 $Jkg^{-1}$ CINE and 972 $Jkg^{-1}$ CAPE[3]. During this specific day, there was no large-scale influence and isolated convective cells could have originated a squall line, extensively studied by Silva Dias et al. (2002) using radar, satellite and modeling.

The second case study is obtained by running the model with a radiosonde from the dry-to-wet season (Morales et al., 2004) on 1800 UTC 18 September 2002 (Figure 1b). This day was chosen to represent a local convection situation, with also minimum large-scale influences. During September 18th, there was a low convective fraction (0.29 – calculated using the reflectivity

3 *Convective Available Potential Energy*: total buoyant energy available per unit mass to an air parcel to rises from the level of free convection to the level of neutral buoyancy for a given atmospheric sounding.

radar images, installed specially for the RaCCI experiments), a reasonable number of lightnings detected by BLND[4] (104 lightnings) and a high CAPE (1440 $Jkg^{-1}$), characterizing an unstable atmosphere.

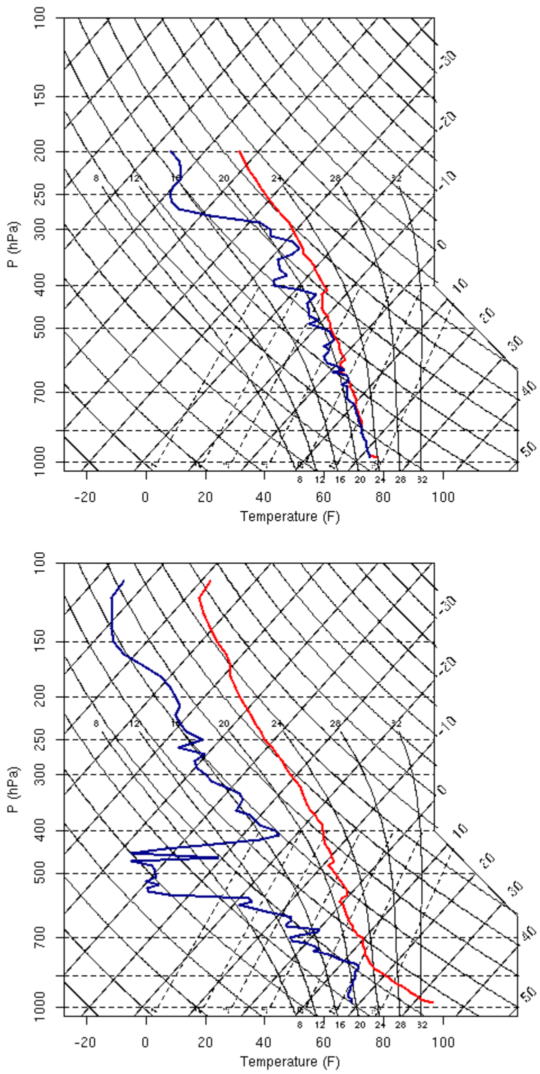


a

b

Figure 1 – SkewT-logP radiosonde diagram for the model initial conditions. Temperature and dew point temperature are denoted by blue and red lines, respectively, and gray dashed lines are moist adiabats. a) 1200 UTC 07 February 1999, and b) 1800 UTC 18 September 2002.

### *3.1 07 February 1999*

Figure 2 shows the time versus height evolution of vertical velocity ( $\overline{w}$ ), variation of the large-scale potential temperature ( $\overline{\theta}$ ), the mixing ratio of the six types of hydrometeors considered in this model ( $\overline{q_x}$ ), and vertical profile of model breakdown electric field, for the simulation using the thermodynamic profile of February 07th, 1999. Since this profile was very humid, there was condensation of cloud water particles ( $\overline{q_{cw}}$ ) inside the boundary layer during the first minutes of the simulation. Moreover, once the profile was humid and unstable, this simulation produced five clouds.

The first cloud had its maximum top at 8 km of height, with maximum updraft of 8.5 $ms^{-1}$ and had the maximums of all hydrometeors simulated, except for the graupel. These maximums were not very high (if compared to the next simulated day – section 3.2), and then did not promote a high potential temperature ( $\overline{\theta}$ ) perturbation (around 0.03 $ms^{-2}$), as tit can be seen in Figure 2. The maximums of $\overline{\theta}$ are due to the latent heat realize during the phase of water transformation (solid to liquid and vice-versa). The first cloud started to precipitate around *t*=20 min, with a maximum in *t*=45 minutes and ending in *t*=52min. None of the types of hydrometeors were completely precipitated, as it can be seen by the continuous decreasing of these values without reaching 0 $gkg^{-1}$ anytime. The ice phase of this cloud were initiated in t=34 min with the formation of hail and graupel, while the formation of snow and ice crystals were observed a minute later. As soon as there was the appearance of graupel and ice crystals in the simulated cloud, it was reached the lightning breakdown of the electric field in 36 minutes of simulation, as shown in Figure 2.

The model was able to produce a reasonable charge transfer between graupel and ice crystals, with electric fields up to ~ -300 and 300 kV/m. The model stopped to calculate the hydrometeor charge transferring, and the hydrometeor kept the same density charges from the moment of lightning to the end of the simulation. However, the water condensation and formation of other clouds continued with a life cycle of around 6 to 7 minutes. This feature of a multiple cloud formation is an evidence of the squall line maintenance dynamic observed by radar and satellite data during this day, and extensively studied by Silva Dias et al. (2002) using a mesoscale model to simulate the situation. Silva Dias et al. concluded that only a few very deep and intense convective cells were necessary to explain the overall precipitating line formation and that discrete propagation and coupling with upper atmosphere circulations may explain the appearance of several lines during this day. They also notice that the topography may be the cause of initial convective development, and that there are indications that the small scale deforestation may have an effect on increasing rainfall in the wet season when the large-scale forcing is very weak.

4 *Brazilian Lightning Detection Network*.

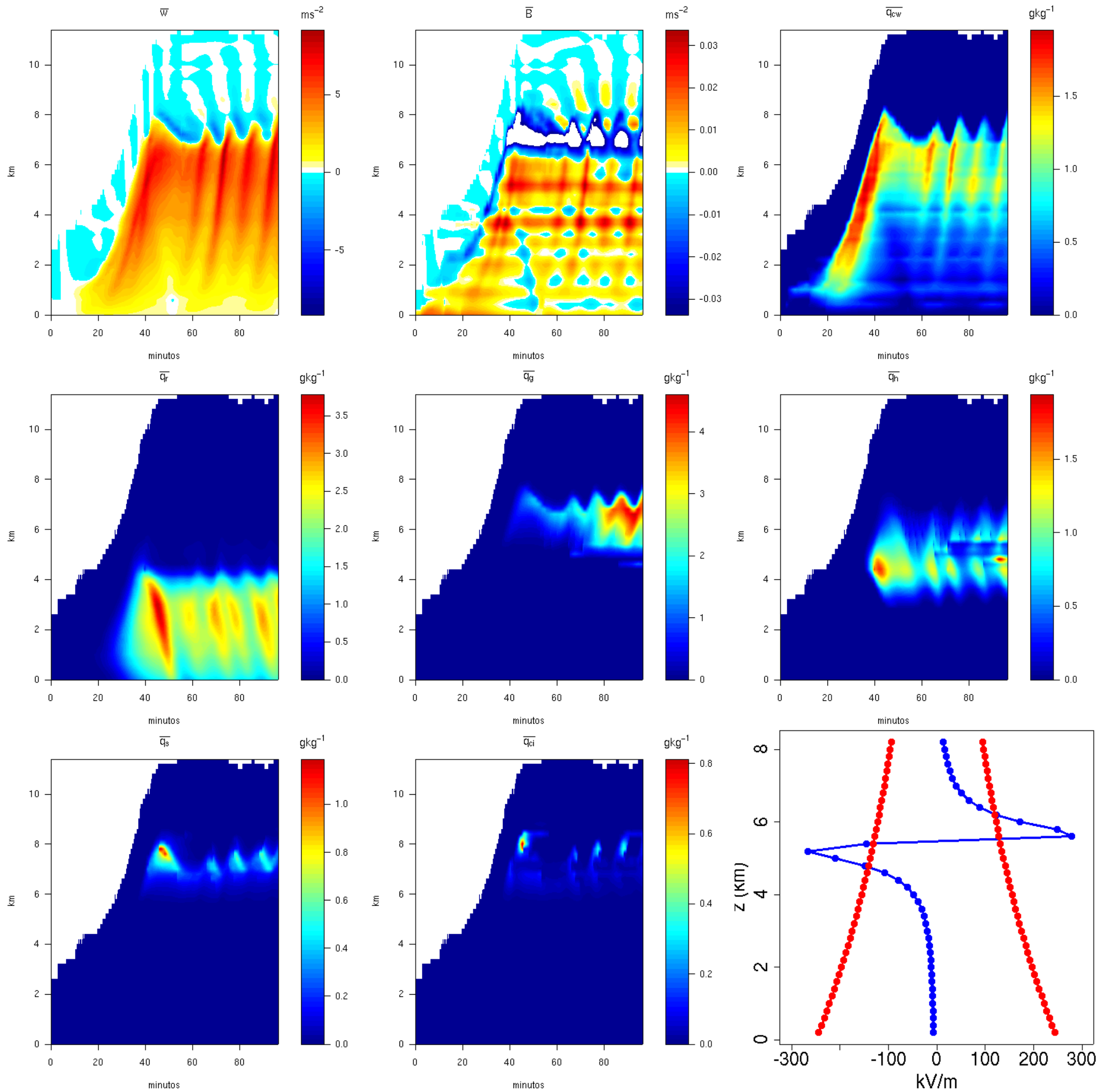


Figure 2 – Temporal evolution of vertical velocity ( $\overline{w}$ ), variation of the large-scale potential temperature ( $\overline{\theta}$ ), the mixing ratio of the six types of hydrometeors considered in this model ( $\overline{q_x}$ ), and vertical profile of model breakdown electric field (kV/m) in t=36 min (blue line) together with the breakeven electric field (red lines) - Equation (11). Values for the simulation with the 07 February 1999 radiosonde.

### *3.2 18 September 2002*

The maximum height of the top of the simulated cloud using the thermodynamic profile of September 18th, 2002, was ~12 km at *t*=48 min. The first cloud droplets ( $\overline{q_{cw}}$ ) were formed in 17 minutes of simulation and the first rain drops ( $\overline{q_r}$ ) appeared 8 minutes later, as it can be seen in Figure 3. The maximum of rain ( $\overline{q_r}=7$ gkg$^{-1}$) was obtained after 37 minutes of simulation, suggesting the contribution of melted hydrometeors (such as graupel and hail) to the achievement of this high value. Precipitation fallout occurred some minutes after the maximum of $\overline{q_r}$ (*t*=45 min).

The cloud ice phase was initiated by graupel, ice crystals and snow flakes (*t*=28 min) due to rain droplets and water vapor that were carried by updrafts above the freezing level (*T*=0ºC, ~4.5 km of height). Only five minutes after the first ice particles were formed, hail is formed with a maximum of 3.8 gkg$^{-1}$. Graupels are smaller particles than hail, therefore they can be found at higher altitudes such as 10 km, while hail was confined bellow 8 km of height. The cloud updrafts reached high levels, above 8 km, initiating ice crystals nucleation. Ice crystals can grow by aggregation of other ice particles or rimming of supercooled cloud droplets, creating the snowflakes and graupels. The maximum of ice crystals (1.6 $gkg^{-1}$) was found some minutes before the maximum of snow (2.4 $gkg^{-1}$) indicating the presence of aggregation and rimming processes. The rapid ice crystals formation at ~ 9.5 km of height is responsible for a high quantity realize of latent heating. This can be seen at the maximum value of $\bar{\theta}=1.5$ °C at the same height and time of maximum $\overline{q_{ci}}$ .

The cloud stopped growing in 48 minutes of simulation, when it can be seen just downdrafts at all vertical profile. However, ice crystals, snowflakes, hail and graupel persisted during a short period of time until they were completely evaporated.

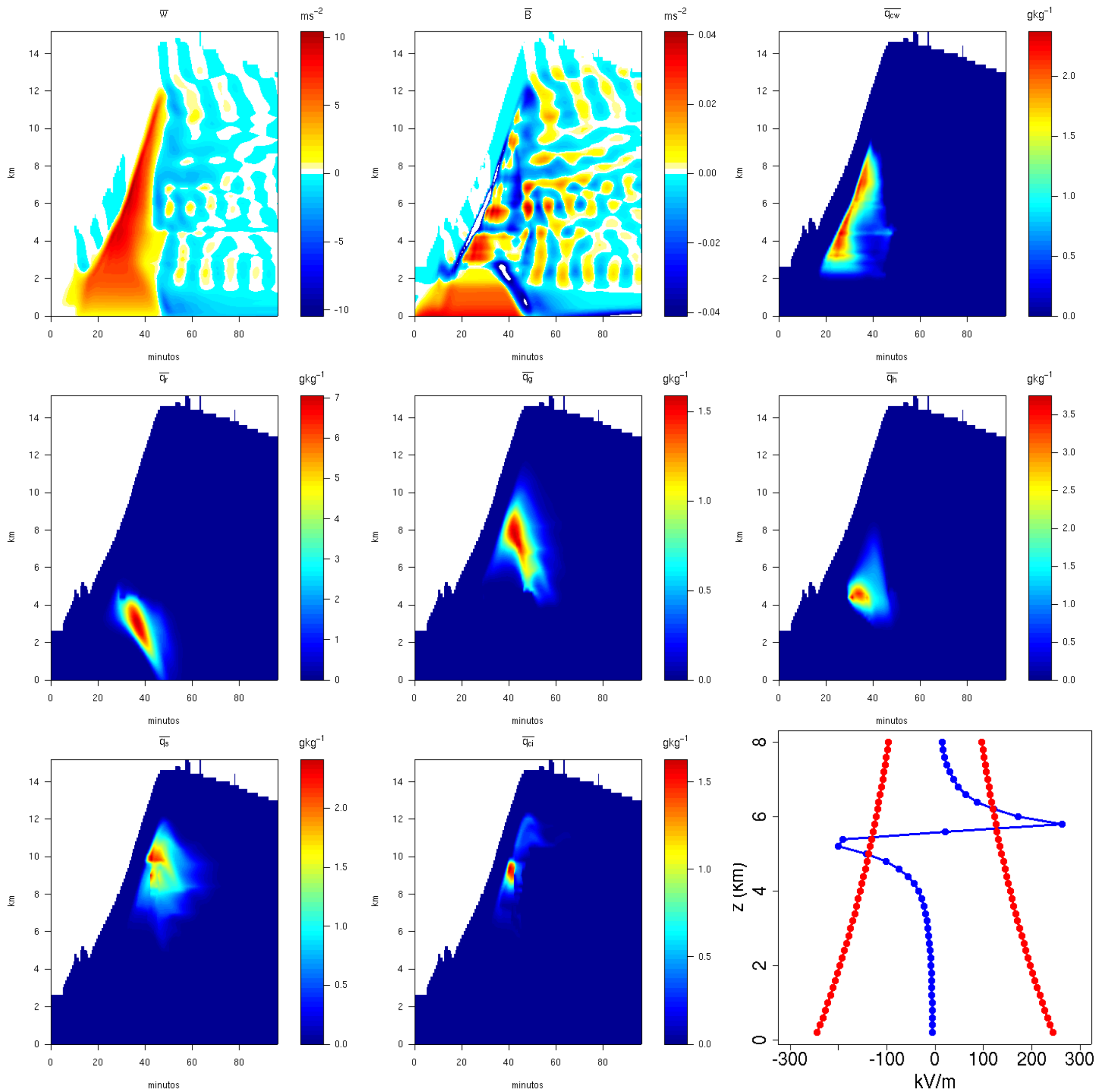


Figure 3 – Temporal evolution of vertical velocity ( $\overline{w}$ ), variation of the large-scale potential temperature ( $\bar{\theta}$ ), the mixing ratio of the six types of hydrometeors considered in this model ( $\overline{q_x}$ ), and vertical profile of model breakdown electric field ( kV/m) in t=28 min (blue line) together with the breakeven electric field (red lines) - Equation (11). Values for the simulation with the 18September 2002 radiosonde.

The charge electrification of hydrometeors in ice phase occurred in a rapid and intense way. Charge transfer was confined to the mixed cloud phase (where there is the presence of ice particles and supercooled cloud droplets, ~4.8 km of height) due to the collision-rebounding mechanism between hail and the few ice crystals and snowflakes present at this level. The negative charging of graupel and hail, and the positive charging of ice crystals and snow at 4.8 km (T ~ -8°C) is coherent with the laboratory work of Takahashi (1984) used in this model. Figure 3 also shows the vertical distribution of the breakdown and breakeven electric field chosen as the limit for lightning to occur. The lightning occurred at the moment of this very high charging, in 28 minutes of simulation. The model was able to produce a reasonable charge transfer between hail, ice and snow, with electric fields up to ~ -270 and 290 kV/m. As soon as there was a lightning, the model stopped to calculate the hydrometeor charge transferring, and the hydrometeor kept the same density charges from the moment of lightning to the end of the simulation.

## 4 DISCUSSION

The cloud model with the dynamic formulation of Ferrier and Houze (1989) and microphysics of iced hydrometeors with electrification proposed by Petersen (1997) reproduced satisfactorily the dynamics and microphysical processes considered. The initial condition reproduced by the temperature and humidity profiles is important for the formation and distribution of hydrometeors here simulated. Together with the low level forcing, these features have an important play in the rapid and efficient conversion of the available humidity into hydrometeors, and then in the charge transfer during collisions, producing reliable breakdown fields and so far lightning.

The main characteristics imposed by the large-scale conditions of the different seasons simulated as case studies were clearly seen, such as a more unstable and humid boundary layer of the wet season that leads to convection easily with a not so strong low level forcing, and the very stable boundary layer of the dry-to-wet period, being a strong barrier for the initiation of the convection. The case studies also simulated reasonably the convection occurred observed by radar and satellite, and studied by other authors (Silva Dias et al., 2002). However, as shown by Albrecht et al. (2005), during the dry-to-wet period, a high CINE together with a moderate CAPE and a strong enough low level forcing, could break the stable boundary layer, and explode into a vigorous cumulonimbus. This feature can be the main reason for number of lightning records along a year. However, this will be still confirmed in the future step of this 1D electrified cloud model, the redistribution of charges after a breakdown, producing several lightnings and a complete thunderstorm life cycle.

The aerosol effect is also an issue to be explored with this model. This can be done by playing with the numbers of the functions that parameterize the water and ice species, making the same amount of mixing ratios to represent different hydrometeor spectra with more or less number of droplets/ice.

Another important part of this work is the identification of all days with only local convection in the region covered by the radars of RACCI field campaign, to study them throughout numerical simulations using this 1D cloud model. Identifying these days, it can be inferred the real effects of each possible forcing that influences cloud electrification: thermodynamic forcing (CAPE), aerosols (number of hydrometeors), topography (rising of low-level air parcels), and large-scale (seasons, divergence of air and humidity).

With a reliable parameterization to be used for continuously charge and discharge hydrometeors, the next step will be to insert a similar parameterization of electrification of clouds into the mesoscale model BRAMS, used in the University of Sao Paulo for weather forecasts. However, BRAMS is a three-dimensional model and therefore there will be also the possibility to calculate the trajectory of lightning discharges inside and outside the cloud (Mansell et al., 2001). Such study is necessary to develop a good understanding of observed relationships between lightning and storm properties that hold promise for nowcasting, storm warnings, lightning forecast, and the global impact of $NO_x$ produced by lightning (which acts as a catalyst in reactions with ozone and so survives to continue affecting ozone concentrations).

## 5 REFERENCES


Albrecht, R. I., C. A. Morales, M. A. F. Silva Dias, W. Petersen, 2005: “Electrified 1D cloud model: Investigation of the Amazonian monsoon and dry-to-wet seasonal conditions for convection”, *Preprints of 11st Mesoscale and 32nd Radar Meteorology Conference*, Albuquerque, NM.

Baker, B., M. Baker, E. R. Jayaratne, J. Latham, and C. P. R. Saunders, 1987: “The influence of diffusional growth rates on the charge transfer accompanying rebounding collisions between ice crystals and hailstones”, *Q. J. Roy. Meteor. Soc.*, 113, 1193-1215.

Baker, M., and J. D. Dash, 1994: "Mechanism of charge transfer between colliding ice particles in thunderstorms", *J. Geophys. Res.*, 99, 10621-10626.

Cheng, S.-H. and W.-Y. Sun, 2002: "A one-dimensional time dependent cloud model", *Journal of Meteorological Society of Japan*, vol. 80, pp. 99-118.

Cheng, S.-H. and W.-Y. Sun, 2004: "An explicit one-dimensional time-dependent tilting cloud model", *Journal of the Atmospheric Sciences*, vol. 61, pp. 2797-2816.

Department of Transportation, Federal Aviation Administration, *Standard, Lightning Protection, Grounding, Bonding, and Shielding Requirements for Facilities*, FAA-STD-019c, Washington D. C., 1999.

Ferrier, B. S. and R. A. Houze, 1989: "One-Dimensional time-dependent cumulonimbus convection", *Journal of the Atmospheric Sciences*, vol. 43, pp. 330-352.

Ferrier, B. S., 1994: "A double-moment multiple-phase four-class bulk ice scheme. Pat I: Description", *Journal of the Atmospheric Sciences*, vol. 51, pp. 249-280.

MacGorman, D. R. and W.D. Rust, 1998: *The electrical nature of storms*, New York, Oxford University Press.

Mansell, E. R., D. R. MacGorman, and J. M. Straka, 2001: "Lightning flash rate and CG polarity relationships in simulated storms", *Eos. Trans. AGU*, vol. 82 (47), Fall Meet Suppl., Abstract AE12A-0088.

Marshall, T. C., M. P. McCarthy, and W. D. Rust, 1995: "Electric field magnitudes and lightning initiation in thunderstorms", *J. Geophys. Res.*, vol. 100, pp. 7097-7103.

Morales, C. A., L. A. T. Machado, M. A. F. Silva Dias, W. Amorim, M. E. B. Frediani, and R. I. Albrecht. 2004: Characteristics of the precipitating systems during the 2002 dry-to-wet field campaign in the Amazon region, *Preprints on XIII Brazilian Metorological Congress*, Fortaleza, CE, Brazil.

Petersen, W., 1997: "*Multi-scale processes studies in the tropics: Results from lightning observations*", Ph. D. dissertation, Colorado State University, Paper No 632, April, pp. 354.

Rickenbach, T. M., R. N. Ferreira, J. Halverson, D. L. Herdies, and M. A. F. Silva Dias, 2002: Modulation of convection in the southwestern Amazon basin by extratropical stationary fronts. *J. Geophys. Res.*, **107**, 8062.

Rosenfeld, D., 1999: TRMM observed first evidence of smoke from forest fires inhibiting rainfall. *Geophys. Res. Lett.*, **26**, 3105-3108.

Saunders, C. P. R., W. D. Keith, and R. P. Mitzeva, 1991: "The effect of liquid water on thunderstorm charging", *J. Geophys. Res.*, vol. 96, pp. 11007-11017.

Silva Dias, M. A. F., W. Petersen, P. L. Silva Dias, R. Cifelli, A. K. Betts, M. Longo, A. M. Gomes, G. Fisch, M. A. Lima, M. A. Antonio, R. I. Albrecht, 2002: "A case study of convective organization into precipitating lines in the Southwest Amazon during the WETAMC and TRMM-LBA", *J. Geophys. Res.,* 107, 8054.

Takahashi, T., 1978 "Rimming electrification as a charge generation mechanism in thunderstorms", *Journal of the Atmospheric Sciences*, vol. 35, pp. 1536-1548.

Takahashi, T., 1984: "Thunderstorm electrification – A numerical study", *J. Atmos. Sci.*, vol. 41, pp. 777-1794.

Williams, E. R., R. Zhang, D. Boccippio, 1994: "Microphysical growth state of ice particles and large-scale electrical structure of clouds, *J. Geophys. Res.*, vol. 99, pp. 10787-10792.

Williams, E. and co-authors, 2002: Contransting covective regimes over the Amazon: implications for cloud electrification. *J. Geophys. Res.*, 107, 8082.